AGU100 ADVANCING EARTH AND SPACE SCIENCE

JGR Atmospheres

RESEARCH ARTICLE
10.1029/2019JD030913

Ice Nucleation by Marine Aerosols Over the North Atlantic Ocean in Late Spring

Elise K. Wilbourn[1], Daniel C. O. Thornton[1], Catherine Ott[2], Jason Graff[3], Patricia K. Quinn[4], Timothy S. Bates[4,5], Raghu Betha[6,7], Lynn M. Russell[6], Michael J. Behrenfeld[3], and Sarah D. Brooks[2]

[1]Department of Oceanography, Texas A&M University, College Station, TX, USA, [2]Department of Atmospheric Science, Texas A&M University, College Station, TX, USA, [3]Department of Botany and Plant Pathology, Oregon State University, Corvallis, OR, USA, [4]NOAA Pacific Marine Environmental Laboratory, Seattle, WA, USA, [5]Joint Institute for the Study of the Atmosphere and Oceans, University of Washington, Seattle, WA, USA, [6]Scripps Institution of Oceanography, University of California, San Diego, La Jolla, CA, USA, [7]Now at Department of Civil, Environmental, and Construction Engineering, Texas Tech University, Lubbock, TX, USA

Key Points:
- Isolated small phytoplankton cells, including *Synechococcus,* picoeukaryotes, nanoeukaryotes catalyze atmospheric ice nucleation
- At seawater concentrations, salts in water droplets inhibit ice nucleation by biological components
- Following a storm-driven mixing event, the mean ice-nucleating temperature of primary aerosol rose from −28.0 ± 1.5 °C to −24.5 ± 0.9 °C

Supporting Information:
- Supporting Information S1
- Figure S1
- Figure S2

Correspondence to:
S. D. Brooks,sbrooks@tamu.edu

Citation:
Wilbourn, E. K., Thornton, D. C. O., Ott, C., Graff, J., Quinn, P. K., Bates, T. S., et al. (2020). Ice nucleation by marine aerosols over the North Atlantic Ocean in late spring. *Journal of Geophysical Research: Atmospheres*, *125*, e2019JD030913. https://doi.org/10.1029/2019JD030913

Received 30 APR 2019
Accepted 10 FEB 2020
Accepted article online 13 FEB 2020

Abstract Here we report the ice nucleating temperatures of marine aerosols sampled in the subarctic Atlantic Ocean during a phytoplankton bloom. Ice nucleation measurements were conducted on primary aerosol samples and phytoplankton isolated from seawater samples. Primary marine aerosol samples produced by a specialized aerosol generator (the Sea Sweep) catalyzed droplet freezing at temperatures between −33.4 °C and − 24.5 °C, with a mean freezing temperature of −28.5 °C, which was significantly warmer than the homogeneous freezing temperature of pure water in the atmosphere (−36 °C). Following a storm-induced deep mixing event, ice nucleation activity was enhanced by two metrics: (1) the fraction of aerosols acting as ice nucleating particles (INPs) and (2) the nucleating temperatures, which were the warmest observed throughout the project. Seawater samples were collected from the ocean's surface and phytoplankton groups, including *Synechococcus*, picoeukaryotes, and nanoeukaryotes, were isolated into sodium chloride sheath fluid solution using a cell-sorting flow cytometer. Marine aerosol containing *Synechococcus*, picoeukaryotes, and nanoeukaryotes serves as INP at temperatures significantly warmer than the homogeneous freezing temperature of pure water in the atmosphere. Samples containing whole organisms in 30 g L^{-1} NaCl had freezing temperatures between −33.8 and − 31.1 °C. Dilution of samples to representative atmospheric aerosol salt concentrations (as low as 3.75 g L^{-1} NaCl) raised freezing temperatures to as high as −22.1 °C. It follows that marine aerosols containing phytoplankton may have widespread influence on marine ice nucleation events by facilitating ice nucleation.

1. Introduction

Pure cloud water droplets form ice crystals homogeneously at temperatures below −36 °C (Hoose & Möhler, 2012; Kanji et al., 2017; Vali et al., 2015). Certain types of aerosol particles, referred to as ice nucleating particles (INPs), can catalyze ice nucleation at lower supersaturations and warmer temperatures. The four mechanisms of heterogeneous ice nucleation are deposition freezing, immersion freezing, condensation freezing, and contact freezing (Hoose & Möhler, 2012; Kanji et al., 2017; Murray et al., 2012; Vali et al., 2015). Contact nucleation occurs when a particle is in contact with the surface of the droplet and induces freezing (Brooks et al., 2014). Immersion freezing occurs when an INP becomes immersed in a droplet and subsequently freezes. Similarly, condensation freezing occurs when an INP becomes immersed in a supercooled droplet and freezing occurs concurrently with droplet formation (Kanji et al., 2017). In contrast, deposition freezing occurs when ice grows directly on the INP from the vapor phase.

Over the North Atlantic Ocean, ice is present in both mixed phase and cirrus clouds (Mace, 2010). Agreement between modeled immersion nucleation and satellite observations of ice water path are better when primary marine aerosols are included as sources of INPs at mixed phase clouds temperatures (Yun & Penner, 2013). Globally, a better understanding of cloud water phase is needed, particularly for mixed phase clouds which form between −15 and −30 °C. For example, when the phase partitioning of cloud water determined by six global climate models and satellite retrievals were compared, the distribution of cloud phase according to temperature varied greatly (Komurcu et al., 2014). In the mixed phase cloud regime

where phase is highly sensitive to the choice of ice nucleation scheme, none of the models predicted realistic cloud phases.

Certain physical characteristics can increase the ice nucleating ability of aerosol particles. Increased particle surface area may lead to warmer ice nucleation temperatures (Fletcher, 1969; Hoose & Möhler, 2012). Hexagonal crystalline structures often act as INPs, facilitating freezing above the threshold for homogenous freezing (Turnbull & Vonnegut, 1952). It was shown by Kiselev et al. (2017) that nucleation on hexagonal structures such as K-feldspar typically occurs on the surface of the hexagonal crystals and especially in cracks. More recently, viscous liquids and glassy solids have been identified as effective INPs (Collier & Brooks, 2016; Murray et al., 2010).

Of the many studies of immersion mode nucleation, a wide variety of aerosol may be described as moderately effective INPs, facilitating freezing at temperatures between 5 and 15 °C warmer than the homogenous threshold temperature (−36 °C) (Hoose & Möhler, 2012; Murray et al., 2012). Relatively few compositions have been characterized as highly effective INP, catalyzing nucleation at temperatures at −5 °C and warmer. Anthropogenic sources of INPs include soot particles and other industrial pollutants (Brooks et al., 2014; DeMott, 1990), while natural INPs can come from a wider range of biological and abiotic sources (Kanji et al., 2017; Schnell & Vali, 1975, 1976) including maritime air masses (Rosinski et al., 1986, 1987). Mineral dusts, especially K-feldspar, are very effective INPs with freezing temperatures as warm as −15 °C (Atkinson et al., 2013). Biological aerosols with ice nucleation potential include pollen (Hader et al., 2014; Pummer et al., 2012), diatoms (Alpert et al., 2011a, 2011b; Wilson et al., 2015), and bacteria (Failor et al., 2017; Kim et al., 1987; Lindow et al., 1978; Maki et al., 1974). The bacteria *Pseudomonas syringae* is one of the most effective known biological INPs, with nucleation observed at temperatures as warm as −1.8 °C (Maki et al., 1974; Wex et al., 2015). Bacteria from several other taxa, including *Lysinibacillus, Xanthomonadaceae, Enterobacteriaceae,* and additional members of *Pseudomonadaceae,* are also capable of acting as biological INPs at temperatures between −2 °C and −8 °C (Failor et al., 2017; Kim et al., 1987; Lindow et al., 1978). Growing interest in this topic has led to a number of observations on the ice nucleating behavior of marine aerosols (Brooks & Thornton, 2018; Creamean et al., 2019; DeMott et al., 2016; Huang et al., 2018; Irish et al., 2017, 2019; Ladino et al., 2016; McCluskey et al., 2017, 2018; Wilson et al., 2015).

Studies of phytoplankton as a source of primary marine aerosols indicate that many phytoplankton and associated organic matter are sources of INPs in immersion and deposition mode (DeMott et al., 2016; Knopf et al., 2011; Ladino et al., 2016; Wilson et al., 2015, Wolf et al., 2019). For example, the diatom *Thalassiosira pseudonana* nucleated ice via immersion at temperatures of −23 °C and via deposition mode at colder temperatures in a laboratory study (Alpert et al., 2011a). In another study, a green alga (*Nannochloris atomus*) was observed to catalyze immersion ice nucleation at temperatures as high as −28 °C, whereas *Emiliania huxleyi* was a poor INP and did not catalyze immersion freezing. In contrast, in deposition mode experiments both were active catalysts. *Nannochloris atomus* activated freezing below −33 °C at ice saturation ratios as low as 1.21, and *Emiliania huxleyi* activated ice at ice saturation ratios as low as 1.19 at temperatures of −23 °C and below (Alpert et al., 2011b). Early work on the ice nucleating ability of phytoplankton-laden seawater was performed by Schnell and Vali (1976). In comparison, seawaters devoid of phytoplankton did not act as INP and facilitate freezing. In another study, Fall and Schnell (1985) surveyed 21 marine phytoplankton cultures and found that one culture, *Heterocapsa niei* PY-5 facilitated freezing above −12 °C, whereas the rest of the cultures facilitated freezing between −19 to −21 °C. It should be noted that these freezing surveys were conducted in buffered media and the presence of salt in the droplets was not accounted for. Wolf et al. (2019) conducted a study on the deposition ice nucleation activity of *Prochlorococcus* and individual compounds selected to represent the organic contents of *Prochlorococcus*. The deposition nucleation efficiency of amylopectin, agarose, and aspartic acid were similar to aerosolized *Prochlorococcus* cultures, suggesting that these components may in part determine the ice nucleation activity of *Prochlorococcus* under cirrus cloud conditions.

In the natural environment, organic matter originating from phytoplankton reaches the atmosphere as a part of sea spray aerosols that are produced by bubble bursting and wave action (Russell et al., 2010; Wilson et al., 2015). The sea surface microlayer (SML) is the thin layer of ocean at the air-sea interface, which is operationally defined as 1 to 1000 μm thick (Engel et al., 2017; Liss & Duce, 1997). Since the SML is selectively enriched in some classes of organic matter relative to the underlying water, it plays an important role

in the introduction of INPs into the atmosphere (Aller et al., 2005, 2017; Chance et al., 2018; Cunliffe et al., 2013; Hunter, 1997; Irish et al., 2017, 2019; Thornton et al., 2016; Zeppenfeld et al., 2019). Enhancement in the concentrations of INPs active between −14 and −27 °C in the SML relative to bulk seawater have been observed in some cases, including Arctic melt ponds and marginal ice zones, (Irish et al., 2019; Zeppenfeld et al., 2019). However, enhancements in SML activity have not been observed in all sampling periods (Irish et al., 2017).

As a phytoplankton bloom progresses, senescence may result in an accumulation of leaky cells, dead cells, and fragments in the SML (Engel et al., 2017; Rahlff, 2019). Cell lysis can also result in a significant release of dissolved organic matter (DOM) into the water (Lenes et al., 2013; O'Dowd et al., 2015; Thornton, 2014). DOM is operationally defined as all organic materials that pass through a GF/F glass fiber filter, which have an average pore size of 0.7 μm, and thus DOM includes small particulates. Heterotrophic bacteria and archaea, while not a source of primary production, play an important role in the consumption and transformation of organic matter fixed by phytoplankton and released into the water (Jiao et al., 2010; Kujawinski, 2011). In addition, processes such as sloppy feeding by grazers (Møller, 2007; Møller et al., 2003) and lytic viral infections (Bettarel et al., 2005; Bratbak et al., 1993; Gobler et al., 1997) contribute significant DOM and particulate organic matter (POM) to the water column. It follows that phytoplankton blooms may emit greater quantities of INPs during periods of bloom decline and collapse.

Measurements of INPs that isolate primary marine aerosols from the total aerosol population are uncommon (Ladino et al., 2016). Marine INP measurements that consider changes in plankton at different locations are also rare (Brooks & Thornton, 2018). Hence, the measurements presented in this study on primary aerosols artificially generated from pristine waters of the North Atlantic Ocean, far removed from coastal influences, help to fill the gap in ice nucleation measurements. Further, an examination of ice nucleation from isolated phytoplankton components of seawater was also performed to compare the ice nucleating ability of aerosols to that of organisms in the ocean's surface waters. The central hypothesis of this study is that phytoplankton, or organic matter aerosol derived from these organisms, represent a population of particles which catalyze atmospheric ice nucleation. Second, the nucleating temperatures and freezing efficiencies of marine INPs may vary depending on the organisms involved. Notably, *Synechococcus* is one of the most abundant and ubiquitous phytoplankton groups, with a global distribution, except in the polar oceans (Partensky et al., 1999; Flombaum et al., 2013), but its potential to facilitate ice nucleation is unknown. The methods employed here enabled different phytoplankton groups, including *Synechococcus*, to be isolated from the environment, and their propensities to contribute to atmospheric ice nucleation processes by immersion freezing were determined. The sampled phytoplankton were representative of in situ conditions, both in terms of assemblage composition and physiological status.

2. Measurements

Atmospheric aerosol and seawater samples analyzed in this study were collected in May 2016 onboard the R/V *Atlantis* during the second NASA North Atlantic Aerosols and Marine Ecosystems Study (NAAMES 2) research cruise. The overarching goal of the series of four NAAMES cruises was to determine links between the seasonal changes in phytoplankton populations and the production of marine aerosols (Behrenfeld et al., 2019). Within the NAAMES framework, the specific objective of this study was to characterize sources and atmospheric ice nucleating potential of marine aerosols.

NAAMES 2 consisted of five sampling stations (Figure 1). The R/V *Atlantis* remained at Stations 1, 2, 3, and 5 for approximately 24 hr and at Station 4 for approximately 96 hr. Multiday sampling at Station 4 was conducted to investigate changes in atmospheric aerosols in the context of the ecosystem responding to a physical perturbation from a storm passing over the region (Graff & Behrenfeld, 2018). During 22 to 24 May, a low pressure storm system moved through the area causing ~9 m wave heights and a deep water entrainment event (NOAA Ocean Prediction Center, http:opc.ncep.noaa.gov/Atl_tab.shtml). The ship arrived on station on 24 May, immediately following the entrainment (Graff & Behrenfeld, 2018). Density, salinity, and temperature were used to estimate the surface mixing layer depth. As discussed in detail by Graff and Behrenfeld (2018), buoyancy frequency calculations and multiple mixed layer depth criteria indicated homogeneous physical properties to well below 200 m upon station occupation with rapid shoaling of the mixed layer to less than 25 m within 24–48 hr of arrival. A profiling Seabird Navis BGCi float and drifter

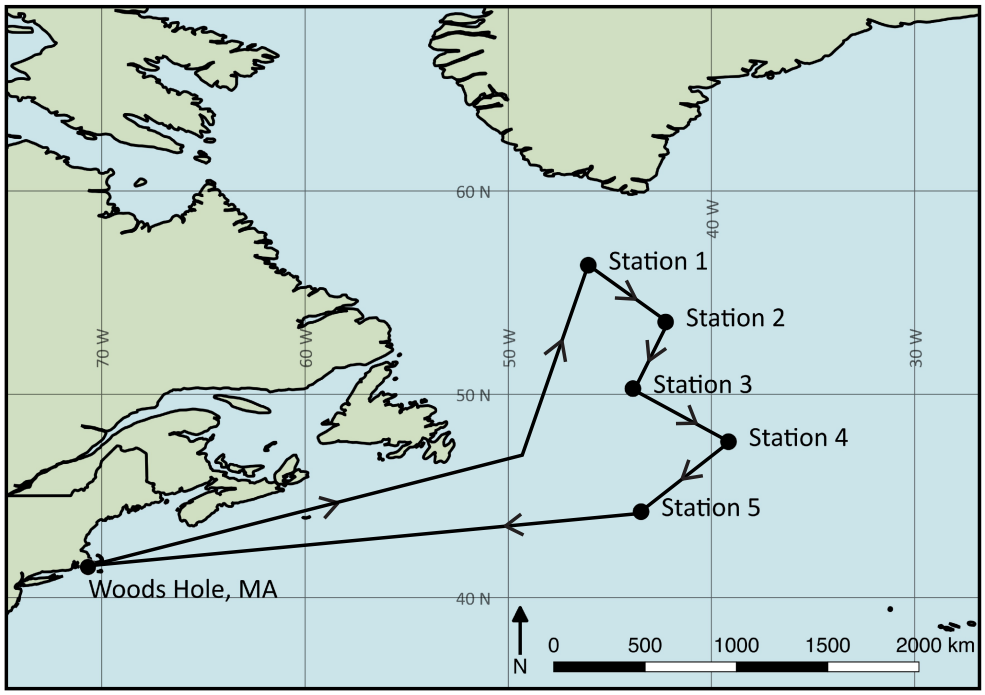

Figure 1. Ship track and sampling locations for the second leg of the North Atlantic Aerosol and Marine Ecosystem Study (NAAMES), which took place during May 2016. The ship stayed at each location for 24 hr with the exception of Station 4, where it stayed for approximately 96 hr.

operated by the University of California, Santa Barbara were deployed immediately prior to the first conductivity, temperature, and depth (CTD) cast and used to track the position of the water mass. Drifter reports (hourly) and float reports (every 7 hr) were used to position the ship in the same water mass for the full 4 days.

This event changed the composition of surface waters available for aerosol production. When strong physical disturbances such as this occur in the ocean waters, phytoplankton communities can be abruptly vertically redistributed over depth. This results in an immediate change in the concentration and composition of the phytoplankton community of the surface layer. Second, the phytoplankton respond to their new environment by making rapid physiological adjustments. Specifically, changes in the availability of sunlight needed for photosynthesis cause phytoplankton to modify their photoacclimation state, resulting in observable changes in the chemical composition of the surface waters through changes in pigments and macromolecules. Graff and Behrenfeld (2018) observed significant increases in both phytoplankton biomass and chlorophyll concentrations in the upper 25 m of seawater at Station 4 over a period of 4 days. These increases, however, did not occur at the same rate, indicating unbalanced growth of different cellular constituents (Shuter, 1979). It follows that changes in both the total biomass and the composition of marine aerosol ejected from these water may occur as well and that these changes may affect ice nucleation.

2.1. Primary Marine Aerosol Collection

Aerosol samples were collected with the Sea Sweep aerosol generator on every sampling day at each station. The Sea Sweep, built at NOAA's Pacific Marine Environmental Laboratory (PMEL), is an aerosol generator designed to replicate primary marine aerosol emissions by bubble bursting mechanisms (Bates et al., 2012). It cannot be said for certain whether the Sea Sweep aerosol generator which we use in this study generated jet drops or film drops. Compressed air was pumped through two coarse stainless steel frits 0.75 m below the ocean surface, causing bubbles to burst at the surface within the sealed hood of the Sea Sweep apparatus. Aerosol-laden flow leaving the Sea Sweep was transported at 1000 L min^{-1} via tubing (5.1 cm inner diameter) to a laboratory van on the 02 deck of the ship where the flow was distributed to a suite of instruments, including a PIXE impaction sampler used to collect samples for evaluation of the aerosols as INPs. The main

sample line (16.7 VLPM) was directed to our instrumentation through a 1 ± 0.2 μm sharp-cut cyclone (SCC 2.229 PM1, BGI Inc., Waltham, Massachusetts). An aliquot of flow, 1 VPLM, was drawn to the PIXE impaction sampler by a diaphragm pump downstream of the impactors. Size-sorted aerosol samples were collected on combusted aluminum foil disks (25 mm diameter) inside PIXE sampler with the L1 and three stages installed to limit the size range to 0.06 to 1 μm diameter, representative of submicron aerosols with the potential to reach the upper troposphere and nucleate ice.

Each sample was collected for approximately 2 hr and immediately frozen at −80 °C, shipped to Texas A&M University on dry ice, and again stored at −80 °C until ice nucleation analysis. All samples were analyzed within 12 months of collection. We note that the time from generation to impaction was less than 20 s, which was insufficient time for secondary aerosols to form. Hence, the Sea Sweep aerosol samples were considered primary marine aerosols (Bates et al., 2012). Primary marine emissions are known to have complex compositions, including contributions from both salt and organic compounds (Barbaro et al., 2019).

The total number of aerosol particles produced by the Sea Sweep was counted using a condensation particle counter (TSI, Inc. Model 3010). Number size distributions were obtained by combining mobility distributions measurements from two Differential Mobility Particle Sizers (DMPS) and applying a data inversion algorithm according to the method of Stratmann and Wiendensohler (1996). In addition to Sea Sweep measurements, the concentration of ambient aerosol sampled directly from an open air inlet was continuously measured by a second TSI 3010 condensation particle counter. Sample air was drawn through an inlet 18 m above the sea surface to the ambient particle counter which was housed in the laboratory van beside instruments sampling the Sea Sweep output. Between stations, the Sea Sweep was removed from the water for travel and was flushed with filtered air before sampling and between each sampling period. Since hours lapse between measurements, any aerosol remaining in the Sea Sweep apparatus and the supply line from the Sea Sweep to the instruments had sufficient time to settle. Bates et al. (2012) found that when sampling air inside the Sea Sweep at times when air was not running to the frits, aerosol counts were less than 20 particles per cubic centimeter. Thus, it is possible, though unlikely, that any aerosol from previous a station sampling periods contaminated samples from a subsequent station.

2.2. Seawater Phytoplankton Cell Collection

Phytoplankton were obtained from surface seawater samples in the surface mixed layer collected via Niskin bottles attached to a CTD rosette on 27 May 2016, the fourth day of Station 4, which represents a stable mixed layer in bloom conditions (Graff & Behrenfeld, 2018). A cell sorting flow cytometer (BD Influx, Becton Dickinson Biosciences) was used to enumerate, classify, and isolate microalgal groups (Graff et al., 2012, 2015; Graff & Behrenfeld, 2018). Cells were sorted based on fluorescence emissions at 692 and 530 nm, and forward and side-scattering intensity. The size ranges 0.5–1, 1–3, and 3–50 μm corresponded to three groups of microorganisms: *Synechococcus,* photosynthetic picoeukaryotes, and photosynthetic nanoeukaryotes (Graff et al., 2015; Sieburth et al., 1978). The flow cytometer was calibrated daily with fluorescent beads (Spherotech, SPHERO^{TM} 3.0 μm Ultra Rainbow Calibration Particles) (Graff & Behrenfeld, 2018). In addition to *Synechococcus*, *Prochlorococcus* is often an abundant cyanobacterium in the open ocean (Flombaum et al., 2013), though generally at lower latitudes in the North Atlantic Ocean than sampled during NAAMES 2 (Baer et al., 2017). *Prochlorococcus* was not present at Station 4 (Graff & Behrenfeld, 2018), therefore, no *Prochlorococcus* sample was produced for the INP analysis. For each sample, approximately 0.2 ml of sheath fluid (30 g L^{-1} NaCl solution (Graff et al., 2012) was enriched with cells in the specified size range to a concentration of approximately 50 cells μL^{-1}. We note that photosynthetic picoeukaryotes and nanoeukaryotes are larger than the upper limit of Sea Sweep aerosols collected by the impactor (1 μm diameter). Nevertheless, they are potential sources of INPs because their cells may leak, lyse, or fragment causing the internal materials and cell fragments to be emitted to the atmosphere (Lenes et al., 2013; O'Dowd et al., 2015).

The sorted seawater samples were stored at −80 °C until ice nucleation analysis at Texas A&M University. In addition, flow cytometry was used throughout the cruise to quantify concentrations of microorganisms in bulk waters collected from the cast of the CTD rosette at the shallowest collection depth (5 m). Samples were immediately passed through the flow cytometer, with between 6,000 and 10,000 cells counted per sample.

2.3. Immersion Mode Ice Nucleation Experiments

Ice nucleation measurements were conducted using a custom ice microscope apparatus built and operated at Texas A&M University (Brooks et al., 2014; Collier & Brooks, 2016; Fornea et al., 2009). The well-established method is described in detail in our earlier work (Fornea et al., 2009) and is outlined briefly here. The major components of the apparatus were an Olympus optical microscope (Model BX51M), sealable Linkam cooling stage (LTS 350), and a digital camera (Q-Imaging Micropublisher 5.0 RTV). Accuracy in temperature control was maintained to within ±0.1 °C by the Linkam stage throughout freeze-thaw cycles from +5 to −40 °C. With this setup multiple ice nucleation data points were determined for each sample.

To set up an experiment, the aluminum foil impaction stage containing a Sea Sweep aerosol sample was placed on a hydrophobic glass microscope slide for support. In this study, experiments were conducted in immersion mode, in which a 2.0 μL drop of HPLC-grade water (VWR) was pipetted onto the center of the impaction stage and directly on top of the potential INPs, which are visible as a small circular spot. In the case of the sorted phytoplankton samples, a 2.0 μL droplet containing sorted organisms was placed directly on a silanized glass microscope slide pretreated with a 1% AquaSil solution (Pierce Chemical Company). The sample was then sealed into the stage and cooled at a rate of 1 °C min^{-1} from 0 to −40 °C. Photographs of the droplet were taken at 400X magnification every 6 s (corresponding to a 0.1 °C temperature change). Once the stage reached −40 °C it was heated at a rate of 5 °C min^{-1} until it reached 5 °C, where the temperature was held for 1 min to ensure complete melting of the droplet. This cooling and warming process was repeated 25 times on the same sample to observe multiple ice nucleation events.

To prevent droplet evaporation throughout the experiment, a humidified flow was generated by combining a flow of saturated nitrogen from a glass bubbler containing ultrahigh purity (UHP) water (0.01 lpm) and a flow of dry nitrogen (0.6 lpm). A hygrometer (EdgeTech DewPrime II, Model 2000) was used to monitor the dew point. Maintaining a dewpoint at approximately −39 °C was optimal for preventing droplet evaporation while ensuring that condensation did not form inside the Linkam stage. In the case of impactor samples collected on aluminum foil substrates, such as the Sea Sweep samples here, the dewpoint must not exceed this setting or condensation onto the foil will occur. Measurements collected with any evidence of condensation were excluded from the data set, resulting in less than 25 cycles in a data set.

After the experimental run, the charge-coupled device camera images were analyzed on a frame-by-frame basis to visibly determine the freezing temperature. All measurements reported in this study met the following quality control criteria: (1) a freezing point was observed during a minimum of three freeze-thaw cycles for the same sample, (2) freezing was clearly observed at a discrete temperature for each observation (i.e., in a single charge-coupled device image), (3) the droplet did not visibly change size, and (4) no condensation was observed adjacent to the droplet on the slide.

The ice nucleating temperature of microorganisms sorted with a flow cytometer was measured from samples collected at Station 4 on Day 4. These samples were representative of the smaller phytoplankton (<50 μm diameter). It is well known that the presence of salt in water extends the temperature range of liquid water to colder temperatures (Bodnar, 1993). Some previous ice nucleation studies (Irish et al., 2017; Wilson et al., 2015), have adjusted the reported ice nucleating temperatures for salt concentration using the AIM model according to the water activity of the salt solution in equilibrium with ice (Koop & Zobrist, 2009). However, a recent study showed that the nucleating temperatures predicted for some compositions are inconsistent with laboratory measurements (Whale et al., 2018). Therefore, rather than make adjustments based on theory, we performed a series of dilutions to measure changes in concentration directly.

Assuming uniform distribution of organisms in the sorted samples (in 30 g L^{-1} NaCl), we estimate that each 2 μL droplet contained approximately 100 cells. Each sample was then diluted with UHP water to the following NaCl concentrations: 15, 7.5, and 3.75 g L^{-1}, resulting in particle counts of 50, 25, and 13 cells, respectively, per 2 μL droplet. Further dilutions were not performed as it was determined that there was a significant possibility that droplets at lower dilutions would contain no cells. Particles were not visible in the microscope photos; therefore, it was not possible to confirm estimated particle counts in the drops.

2.4. Seawater Pigment Analysis

Samples for pigment analysis were collected from the 5 m Niskin bottle on the rosette. High Performance Liquid Chromatography (HPLC) was used to quantify individual phytoplankton pigments (Hooker et al., 2005; Van Heukelem & Thomas, 2001). HPLC provides a precise measurement of chlorophyll *a* concentration in the surface water, coupled to measurements of accessory pigments that may be used as biomarkers for specific groups of phytoplankton. Casts were made between 8:00 and 9:00 a.m. (local time), with the exception of the cast at Station 1, which was made at 12:20 p.m. For pigment analysis, a known volume of sample (1 to 3 L) was filtered with combusted GF/F filters and stored at −80 °C until analysis at the NASA Goddard Space Flight Center Ocean Ecology Laboratory (Greenbelt, Maryland). Pigments were extracted in methanol and analyzed on a 4.6 × 150 mm HPLC Eclipse XDB column using an Agilent RR1200 HPLC system (Agilent Technologies). In addition, vertical profiles of chlorophyll *a* concentration with depth were made for the upper 200 m using samples collected from the Niskin bottles on the CTD rosette. These water samples were filtered, extracted with 90% acetone, and chlorophyll *a* concentrations were measured using a Turner Designs AU-10 fluorometer according to the methods outlined in Mueller et al. (2002).

3. Results and Discussion

3.1. Phytoplankton Bloom After a Storm

Station 4 was occupied for approximately 96 hr. Temperature and chlorophyll *a* depth profiles measured each day at Station 4 are shown in Figure 2. Chlorophyll *a* concentrations were consistent with reestablishment of a phytoplankton bloom following storm-driven mixing. Temperature measurements showed warming of surface waters over the 4 days, resulting in a distinct thermocline from the surface to 25.5 m at Station 4 on Day 3 (Figure 2c), which increased in depth to 49 m on Day 4. On Day 1, chlorophyll *a* concentration was relatively constant (approximately 0.5 mg m^{-3}) throughout the epipelagic zone (Figure 2a). Surface chlorophyll *a* concentration increased to a maximum of 1.9 mg m^{-3} at 13.6 m depth on Day 4 (Figure 2d). For more details on bloom reestablishment processes and the phytoplankton response to the mixing event that occurred at this station and phytoplankton activity, see Graff and Behrenfeld (2018).

3.2. Primary Marine Aerosols as Ice Nucleating Particles

For each Sea Sweep aerosol sample, the droplet sample setup underwent a series of up to 25 freeze-thaw cycles. Due to issues of condensation on the aluminum substrates used to collect field samples, some experimental runs contain fewer data points than obtained in previous laboratory studies conducted on silanized glass microscope slides (Brooks et al., 2014; Collier & Brooks, 2016; Fornea et al., 2009). Ice nucleation measurements on HPLC-grade water droplets on the aluminum substrates used in the PIXE impactor were performed to test for any influence of the substrate on freezing temperatures. The average nucleation temperature was 33.5 ± 2.0 °C, in agreement with the water droplet freezing on the silanized glass slides. The ice nucleation results are summarized in Figure 3 and Table 1.

Mean freezing temperatures ranged from −24.5 ± 0.9 °C on Day 4 of Station 4 to as low as −33.4 ± 1.2 °C on Day 3 of Station 4. Similar to our previous studies, a fairly high degree of variability was observed from one freezing event to the next, with individual freezing events occurring at temperatures as high as −21.4 °C and as low as −35.4 °C. The mean freezing temperature of Station 4 was −25.1 °C. The freezing temperature on the fourth day on Station 4, −24.5 ± 0.9 °C, was the warmest and was statistically different (at the 95% confidence limit) from the three days prior (Days 1–3). The Station 4 Day 4 freezing temperature was also the highest mean temperature observed throughout the cruise and was statistically different at the 95% confidence limit than the mean freezing temperature for all days at other stations with the exception of Station 2, −26.2 ± 1.2 °C.

To determine the concentration of ice-active aerosols (those that freeze) relative to the total sample concentration, the probability of freezing, or fraction frozen, was calculated as

$$P(T) = \frac{\boldsymbol{N_f}}{\boldsymbol{N_o}}, \tag{1}$$

where N_0 is the total number of unfrozen water droplets (including the initial unfrozen droplet and subsequent thawed droplets) and N_f is the number of water droplets frozen at temperature, T (Brooks

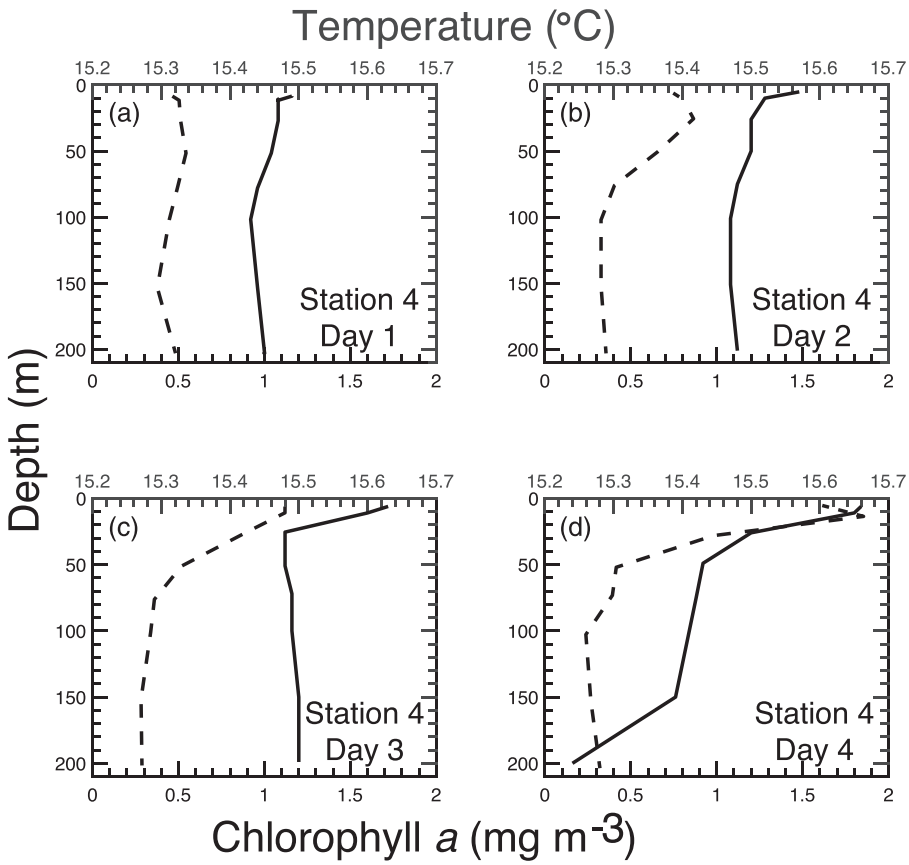

Figure 2. Daily chlorophyll *a* and temperature depth profiles in the upper 200 m of the water column at Station 4. Chlorophyll *a* is plotted with a dashed line, while surface seawater temperature is plotted with a solid line. Panels (a) through (d) represent Days 1–4 of Station 4, respectively. Temperature was measured by the CTD thermometer and chlorophyll *a* by fluorescence after extraction of pigments with 90% acetone from samples collected in Niskin bottles at all available CTD depths.

et al., 2014; Collier & Brooks, 2016; Shaw et al., 2005). The fraction frozen for each sample is shown in Figure 4. In cases when multiple samples were available, all individual data points were compiled into a single data set and the fraction frozen was derived from the compilation. Broadly speaking, the aerosols available to act as INPs were the least efficient nucleators (characterized by the lowest fractions frozen) on the first three days at Station 4. In contrast, the most effective nucleators, with the highest fraction frozen at nearly all temperatures, were observed on Day 4 of Station 4. At the warmest observed droplet freezing temperature, −21.4 °C, freezing was only observed for Station 5. At the intermediate temperature of −25 °C, the fraction frozen for Station 4 Day 4 was 0.69, whereas the fraction frozen for both Days 2 and 3 was 0.0.

The mean ice nucleation temperatures for Stations 1–5 indicate that marine sources produce moderately efficient INPs in general agreement with recent marine INP measurements in other locations (DeMott et al., 2016). The range in freezing temperatures is narrower than reported in other marine INP studies (DeMott et al., 2016; Wilson et al., 2015), perhaps because the Sea Sweep generates exclusively primary marine aerosol with no local secondary aerosol and no continental aerosol influences. Some previous measurements on aerosols classified as marine INPs have observed freezing at higher temperatures than observed here, −27.5 to −6 °C (DeMott et al., 2016). However, it was later noted that all measurements above −12 °C were collected from onshore sampling sites in Puerto Rico and are likely influenced by continental sources of INPs (Brooks & Thornton, 2018). Highly effective marine INPs with immersion freezing temperatures as warm as −5 °C were also observed in aerosol samples collected over the Bering Sea, albeit for much larger aerosols (3 to >12 μm diameter) than sampled in the current study (Creamean et al., 2019). In

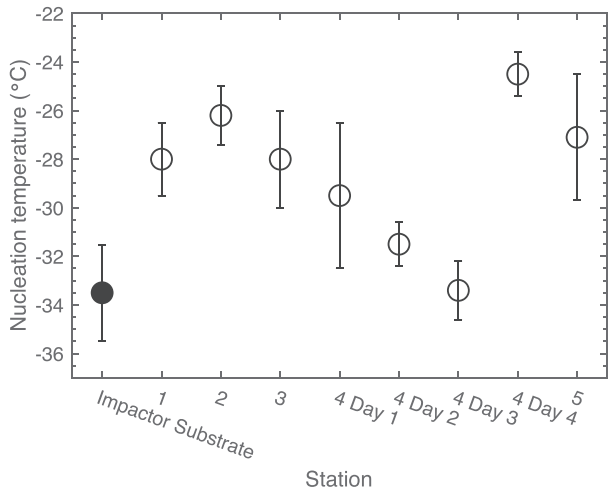

Figure 3. Mean immersion ice nucleation temperatures for Sea Sweep aerosol samples are shown as open circles. Error bars represent the pooled standard deviation. For comparison, the nucleation temperature on a field blank (precleaned Al foil PIXE substrate) is shown as a solid circle).

comparison, we observed freezing at −21.5 °C and below for Sea Sweep samples (0.06 μm to 1 μm diameter). While the reason for this difference cannot be determined for certain, a clear difference is the size of the aerosol tested as potential INP. An additional contributing factor may be regional differences in the composition of the marine aerosols available to act as INPs. The possibility also exists that a low concentration of large aerosols with high ice nucleation potential were present during NAAMES but not sampled with our technique. In a separate study (Mason et al., 2016), the ice nucleation propensity of aerosols collected in the Labrador Sea and several continental locations in a range of sizes between 0.1 and 10 μm diameter were determined. Supermicron aerosol samples which nucleated ice at temperatures of −15 °C or colder represented a significant fraction of the total observed INP.

For reference, the aerosol concentrations and size distributions observed during Sea Sweep deployment are discussed in the supporting information and Figure S2. It should be noted that the absolute concentration of aerosols generated by the Sea Sweep varies with instrument operation and does not provide a measure of ambient aerosol concentration or size distribution. Over the course of the campaign, Sea Sweep aerosol concentrations generated by the Sea Sweep were 2.3–17.2 times greater than ambient aerosol concentrations, with the highest concentrations produced at Station 2. By comparison, the size distributions and mean diameters of generated aerosols were much more consistent than concentrations. Given that the high INP freezing temperatures on Station 4 Day 4 do not coincide with high aerosol loading on the impaction stage or a change in generated size distribution, we conclude that the warmer observed nucleation temperature is likely due to a change in aerosol composition rather than a sampling artifact. In addition, the ambient aerosol concentration was relatively low on Station 4 Day 4, indicating that the warmer freezing temperatures did not coincide with an increase in aerosol concentration.

To compare changes in INP activity with the composition of the underlying seawater, we first inspected the time series of INP freezing temperatures and the corresponding time series of daily mean chlorophyll

Table 1
Pooled Mean Freezing Temperatures and Pooled Standard Deviation for Sea Sweep Aerosol Samples at Each Station

Station number	Date	Lat.	Long.	No. of samples	No. of ice nucleation temp. data points	Mean nucleation temp. (°C) and standard deviation
Station 1	18 May	56°20′ 25.56″	46°3′ 37.80″	2	22	−28.0 ± 1.5
Station 2	20 May	53°33′ 3.84″	42°15′ 25.08″	2	16	−26.2 ± 1.2
Station 3	22 May	50°16′ 36.54″	43°51′ 58.20″	2	15	−28.0 ± 2.0
Station 4, all days	24–27 May	47°40′ 0.72″	39°9′ 55.86″	7	47	−25.1 ± 1.5
Station 4, Day 1	24 May	47°40′ 0.72″	39°9′ 55.86″	2	9	−29.5 ± 3.0
Station 4, Day 2	25 May	47°40′ 0.72″	39°9′ 55.86″	1	3	−31.5 ± 0.9[a]
Station 4, Day 3	26 May	47°40′ 0.72″	39°9′ 55.86″	2	6	−33.4 ± 1.2
Station 4, Day 4	27 May	47°40′ 0.72″	39°9′ 55.86″	2	29	−24.5 ± 0.9
Station 5	29 May	44°13′ 32.88″	43°27′ 59.10″	2	10	−27.1 ± 2.6
Impactor substrate	N/A	N/A	N/A	9	60	−33.5 ± 2.0

[a]Due to limited sample availability, mean and standard deviation were not pooled in this case.

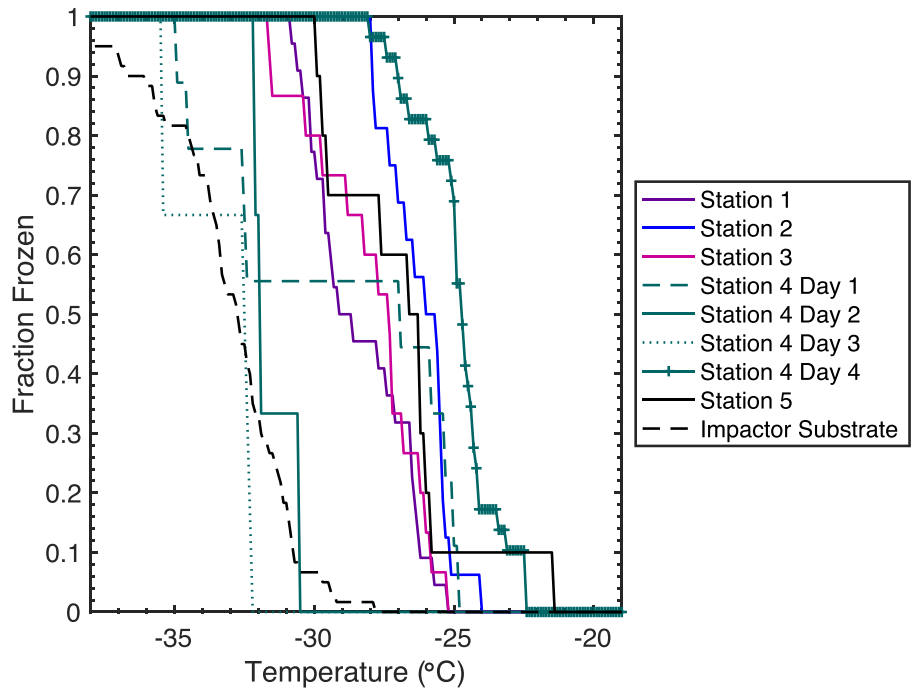

Figure 4. Fraction frozen (fraction of independent observations of sample freezing as a function of temperature). Each data set represents the fraction frozen for a single day of sampling.

concentrations in Figure 5. In Figure 5a, the fraction of sea sweep aerosols frozen by the moderate temperature of −25 °C or warmer are shown. For comparison, the concentration of chlorophyll *a* is shown in Figure 5b. Concentrations of chlorophyll *a* varied substantially throughout the cruise, ranging from 0.39 to 3.47 mg m^{-3} with the highest values observed at Station 3 and lowest on the first day of Station 4. No relationship between chlorophyll *a* and fraction frozen (>25 °C) was evident in the data. There are several studies that have looked for a relationship between chlorophyll *a* concentration and INP production, and a consistent relationship was not reported across these studies (DeMott et al., 2016; Irish et al., 2019; McCluskey et al., 2017). In a mesocosm study, a positive relationship was found between chlorophyll *a* concentrations and INP concentrations at −26 and −30 °C but not at warmer temperatures (DeMott et al., 2016). McCluskey et al. (2017) report a lag between the highest INP concentrations active between −15 and −25 °C and chlorophyll *a* concentrations. In contrast, Irish et al., 2019 did not find a clear link between INP concentrations and chlorophyll *a* concentrations measured in the SML and bulk seawater in the Canadian Arctic. However, the possibility remains that certain components such as small phytoplankton are injected into the atmosphere and remain there long enough to induce freezing events. This subset of smaller marine organisms (<50 μm diameter) includes a widely abundant single celled cyanobacteria, *Synechococcus*, as well as photosynthetic picoeukaryotes, and photosynthetic nanoeukaryote cells.

3.3. Community Composition

The concentrations of *Synechococcus,* picoeukaryotes, and nanoeukaryotes in sea water collected at 5 m depth during the daily CTD casts (taken between 8:00 am and 12:20 p.m. local time) were determined by flow cytometry (Figure 6) and, collectively, represent the smaller chlorophyll-containing cells observed during the project. A complex and variable concentration of other chlorophyll-containing organisms were present as indicated by HPLC pigment data, discussed in the supporting information. The phytoplankton measured by flow cytometry (<50 μm diameter) at the first four stations were dominated by picoeukaryotes in term of abundance, ranging from 52% during Station 3 to 85% during Day 4 of Station 4. *Synechococcus* concentrations increased from 2.76×10^6 L^{-1} on Day 1 of Station 4 to 9.24×10^6 L^{-1} on Day 4, while picoeukaryotes increased from 1.17×10^7 ml^{-1} to 9.13×10^7 L^{-1}, and nanoeukaryotes increased from 5.17×10^5 to 3.68×10^6 L^{-1}. However, on Station 5, *Synechococcus* dominated in terms of abundance, with concentrations

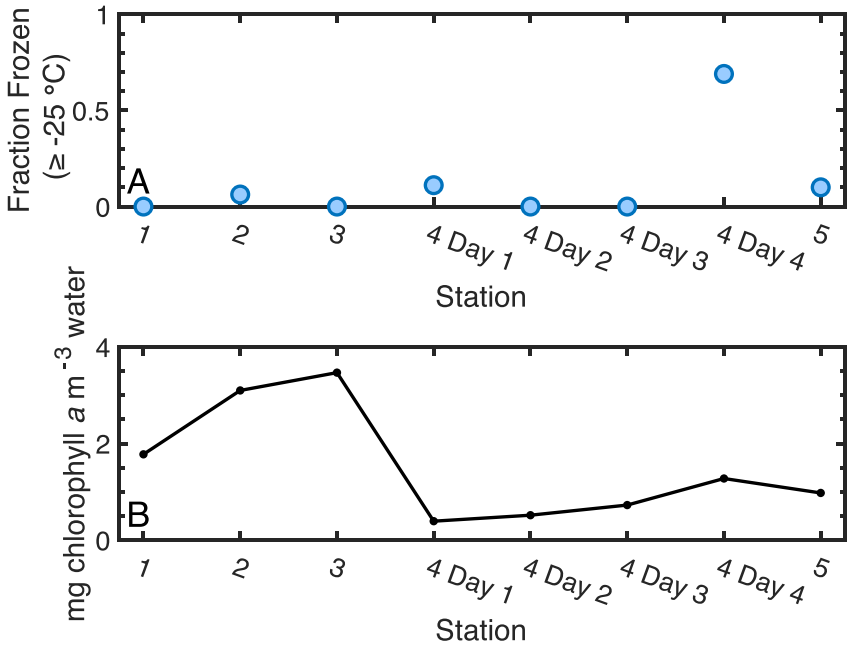

Figure 5. Changes in INP properties and phytoplankton biomass with sampling station. (a) The fraction of droplets frozen at −25 °C or warmer. (b). Surface (5 m depth) chlorophyll *a* concentrations (mg m^{-3}), measured with High Performance Liquid Chromatography (HPLC) from samples collected at 5 m during CTD casts made between 8:00 and 9:00 a.m. local time, with the exception of Station 1, which was made at 12:20 p.m.

of 6.01×10^7 L^{-1}, while concentrations of picoeukaryotes and nanoeukaryotes were relatively low, at 2.64×10^7 and 3.02×10^6 L^{-1}, respectively.

Over the course of the 4 days on Station 4, there was less than a 5% difference in the relative proportions of *Synechococcus*, picoeukaryotes, and nanoeukaryotes. For each organism type, the biggest increases were between Days 3 and 4. Over this period, the fraction of droplets frozen by −25 °C increased from 0.11 on Day 1 of Station 4 to 0.69 on Day 4 and chlorophyll *a* (determined by HPLC) rose from 0.39 mg m^{-3} on Day 1 to 1.28 mg m^{-3} on Day 4.

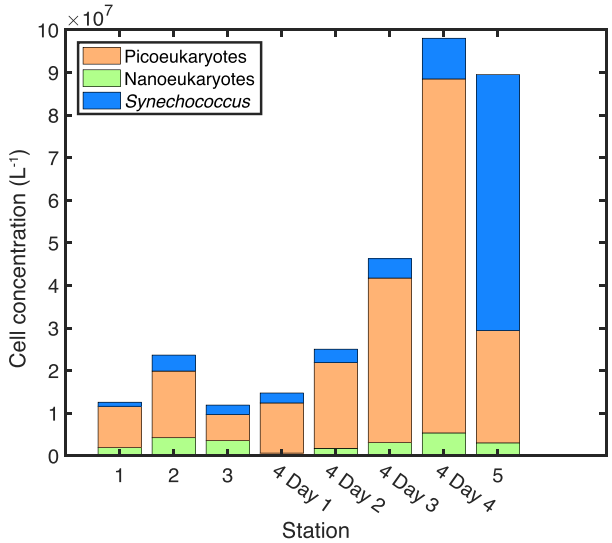

Figure 6. Bulk water cell concentrations sorted using the rapid sorting flow cytometer (BD Biosciences Influx Cell Sorter). Bulk water was taken from the 5 m Niskin bottle taken by CTD cast. Picoeukaryotes (1–3 μm) are represented in orange, nanoeukaryotes (3–50 μm) in green, and *Synechococcus* (0.5–1 μm) by blue.

Both the increase in total cell concentration and the increase in picoeukaryote concentration paralleled the increase in INP activity (represented by the fraction frozen at −25 °C (Figure 5a) between Days 3 and 4 of Station 4). However, moving to Station 5, the picoeukaryote concentration dropped along with the reduction in fraction frozen, while the *Synechococcus* increased to the highest observed concentration throughout the cruise (Figure 6). The groups isolated here represent a possible source of INPs. *Synechococcus* (0.5–1 μm cell diameter) may be present in the Sea Sweep samples as a whole organism. In contrast picoeukaryotes, and nanoeukaryotes (size ranges of 1–3 and 3–50 μm diameter, respectively) would not be sampled by the Sea Sweep. Additional sources such as heterotrophic bacteria and other organic material in the water may also be part of the primary marine aerosols produced over the seawater.

3.4. Phytoplankton Cell Samples as Ice Nucleating Particles

Next, we consider the ice nucleation temperatures of the cytometer-sorted seawater components *Synechococcus,* picoeukaryotes, and nanoeukaryotes individually. Pooled mean freezing temperatures and pooled

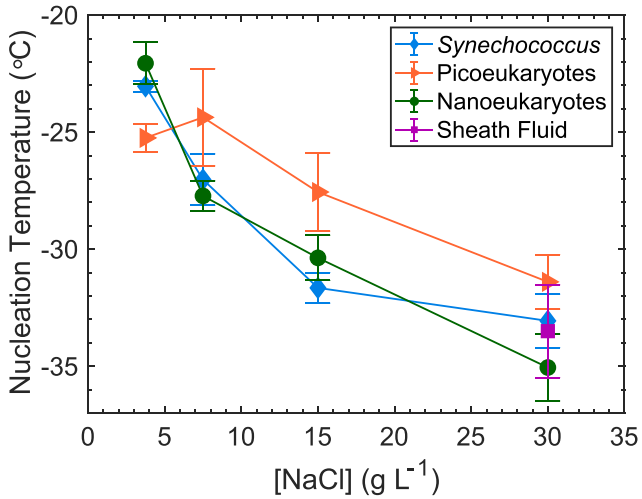

Figure 7. Mean immersion ice nucleation temperatures for sorted seawater samples. All samples were collected on Day 4 of sampling at Station 4 and sorted by the flow cytometer. *Synechococcus* is represented by blue diamonds, picoeukaryotes by orange triangles, and nanoeukaryotes by green circles, with error bars representing the pooled standard deviation. For comparison 30 g L^{-1} NaCl sheath fluid is indicated as a purple square. *Synechococcus,* picoeukaryotes, and nanoeukaryotes had the following size ranges, respectively: 0.5–1, 1–3, and 3–50 μm diameter.

standard deviations for sorted sea water samples are summarized in Figure 7 and Table 2.

Among the 30 g L^{-1} NaCl samples, the warmest freezing occurred at −33.1 ± 1.0 °C for the *Synechococcus* samples, but there was no statistical difference between the three types of organisms in 30 g L^{-1} NaCl (95% confidence level). The temperature of homogeneous nucleation of pure water on a silanized glass microscope slide has been identified at −33.1 °C ± 0.6 °C standard deviation in our apparatus. In all three cases, we observed near-homogeneous freezing temperatures, suggesting only weak ice-nucleating properties of the microorganisms. However, the implications of these results in 30 g L^{-1} NaCl are inconclusive since the presence of the NaCl may inhibit nucleation relative to pure water. For comparison, ice nucleation of the sheath fluid into which organisms were collected (30 g L^{-1} NaCl in deionized water supplied by the Barnstead deionized water system used on the ship) were also conducted. This sheath fluid was used for collection and storage of all *Synechococcus*, picoeukaryotes, and nanoeukaryotes. The sheath fluid froze at −32.4 ± 1.0 °C, which is slightly higher than expected for salt water but can be attributed to the presence of trace amounts of organics present in the deionized water source.

Figure 7 shows that overall trends toward warmer freezing temperatures were observed for each class of microorganism as salt content and cell concentrations decreased. The only exception was that the 3.75 g L^{-1} NaCl samples containing picoeukaryotes had a slightly lower freezing temperature than the 7.5 g L^{-1} NaCl containing picoeukaryote samples. The increase in freezing temperature varied between microorganism type, with the nanoeukaryotes showing the largest change from −33.8 ± 1.5 °C at 30 g L^{-1} NaCl to −22.1 ± 0.9 °C at 3.75 g L^{-1} NaCl. Freezing data from each of the three groups of phytoplankton (*Synechococcus,* nanoeukaryotes, and picoeukaryotes) showed a statistically significant difference (95% confidence interval) between the 30 g L^{-1} NaCl data and the 3.75 g L^{-1} NaCl data. Additional dilutions were not conducted due to the lack of available sample and a concern that as salt content approaches that of pure water the microorganisms may lyse. It should be noted that lysing due to the dilutions performed here cannot be ruled out.

The approximate salt content of freshly formed sea spray is 30 g L^{-1} NaCl. However, during cloud formation, atmospheric particles rapidly uptake water and become more dilute. Assume that a sea spray droplet contains an initial NaCl mass of 10^{-19} kg (Wallace & Hobbs, 2006) and that the droplet activates as a cloud condensation nucleus (CCN), followed directly afterward by immersion freezing of the CCN. In this case, the droplet would have a radius of 0.15 μm at the point of immersion freezing (Lohmann et al., 2016; Wallace & Hobbs, 2006), and the salt content would be reduced to approximately 1.1 g L^{-1} NaCl. In a saturated marine environment, the majority of sea spray droplets will be diluted to at least this level. However, not all of the droplets will freeze immediately. Unfrozen droplets will continue to grow and dilute and may freeze, provided that they contain adequate INP. Conversely, an exception can occur, when the initial sea spray particles are larger than the activation diameter, ice nucleation may occur without any dilution. In summary, sea spray droplets may be present in a broad range of dilutions, with the majority diluted to 1.1 g L^{-1} and lower NaCl concentrations.

Therefore, of the experiments conducted in this study, the freezing temperatures of samples at 3.75 g L^{-1} NaCl may be considered as a lower limit to the temperature which needs to be reached for actual marine drops (containing the identified microorganisms) to freeze. At 3.75 g L^{-1} NaCl, *Synechococcus*, picoeukaryotes, and nanoeukaryotes samples froze at −23.0 ± 0.2, −25.2 ± 0.6, and −22.1 ± 0.9, respectively. These temperatures are well above the temperature of homogenous freezing, −36 °C. Assuming the trend in ice nucleation temperatures observed in our measurements continues, further dilution of the salt would allow freezing to occur at warmer temperatures. Thus, we conclude that marine aerosols containing *Synechococcus,* picoeukaryotes, and nanoeukaryotes in dilute salt solution are modestly effective INPs.

Table 2
Pooled Mean Freezing Temperatures and Pooled Standard Deviations for Flow Cytometer Sorted Sea Water Samples

INP composition	NaCl content (g L^{-1})	Particle concentration (cells per droplet)	No. of samples	No. of ice nucleation data points	Mean nucleation temp. (°C) and standard deviation
Synechococcus	30	100	5	74	−33.1 ± 1.0
Synechococcus	15	50	2	26	−30.2 ± 0.5
Synechococcus	7.5	25	1	13	−27.0 ± 1.1
Synechococcus	3.75	13	1	15	−23.0 ± 0.2[a]
Nanoeukaryotes	30	100	6	92	−33.8 ± 1.5
Nanoeukaryotes	15	50	1	7	−30.4 ± 1.0[a]
Nanoeukaryotes	7.5	25	2	19	−26.2 ± 1.0
Nanoeukaryotes	3.75	13	1	6	−22.1 ± 0.9 [a]
Picoeukaryotes	30	100	4	93	−31.8 ± 1.1
Picoeukaryotes	15	50	1	6	−27.6 ± 1.7 [a]
Picoeukaryotes	7.5	25	1	23	−24.4 ± 2.1[a]
Picoeukaryotes	3.75	13	1	25	−25.2 ± 0.6 [a]
Sheath fluid	30	0	3	45	−32.4 ± 1.0

[a]Due to limited sample availability, mean and standard deviation were not pooled in this case.

These freezing temperatures fall within the range of the freezing temperatures of the Sea Sweep aerosolized samples collected at the same time (freezing temperatures of −33.4 to −24.5 °C).

Flow cytometer sorting provides a limit on the size of organism considered, with an upper limit of ~50 μm (nanoeukaryotes). In a previous ice nucleation study conducted in the Canadian Arctic, samples of bulk sea water and the sea surface microlayer were filtered through PTFE filters with 10, 0.2, and 0.02 μm pore sizes (Irish et al., 2017). In the unfiltered bulk water and microlayer samples, a wide range of freezing temperatures were observed, with peak temperatures significantly higher than those observed in our study. While the possibility that larger organisms present at Station 4 also possess the physical properties conducive to nucleate ice, it is less likely that they will be present in the atmosphere due to low abundance in the ocean and their higher settling velocities. In fact, observations of sea spray diameters include particles ranging from 0.1 to 100 μm diameter (Blanchard & Woodcock, 1957), but the mean diameter is small (0.1 μm) (Clarke et al., 2006). In the Irish et al. (2017) study, the freezing capacity of many (though not all) samples was significantly reduced after filtration, suggesting that the majority of INPs were between the sizes of 0.2 and 0.02 μm. While the possibility cannot be ruled out entirely, it is unlikely that larger particles and/or organisms represent a major unsampled marine INP source in our study.

4. Conclusions

At present, global coverage of INP measurements lack data from many locations. Our measurements indicate that North Atlantic aerosols have ice-nucleating temperatures between −22.4 and −35.4 °C, broadly consistent with the ice-nucleating properties of marine aerosol sampled in other clean marine locations (DeMott et al., 2016; Irish et al., 2017, 2019; McCluskey et al., 2017; Wilson et al., 2015). In addition, this study provides marine INP measurements coordinated with detailed biological sorting by flow cytometry.

Using a flow cytometer we separated particles based on both fluorescence and size to isolates different groups of phytoplankton from the bulk water and other particles such as detritus. Ice nucleation measurements on these samples indicate three specific categories of phytoplankton (*Synechococcus*, picoeukaryotes, and nanoeukaryotes) are moderately effective INPs. The ice nucleating activity of these three isolated types was observed to be very similar. Given that the cyanobacterium *Synechococcus* is one of the most abundant and ubiquitous phytoplankton taxa in surface waters of the ocean (Flombaum et al., 2013), it may have widespread influence on marine ice nucleation and mixed phase cloud formation. Our measurements also demonstrate that the ability of freshly generated spray aerosol to initiate freezing at warm temperatures is counterbalanced by the presence of sea salt until dilution by atmospheric water uptake occurs.

Our Sea Sweep aerosol measurements are the first series of INP measurements conducted on aerosol samples collected over the course of the reestablishment of a phytoplankton bloom after storm induced deep mixing. Interestingly, the daily mean freezing temperature and concentration of particles frozen at −25 °C or warmer were both significantly elevated on the fourth day of observations at a fixed sampling site (Station 4), in parallel with the reestablishment of a phytoplankton bloom. At Station 4, the warmest INP freezing temperatures were observed when the phytoplankton biomass was greatest, both in terms of chlorophyll *a* concentrations measured with HPLC from samples taken at 5 m depth (Figures 5b and S1) and the abundance of small (<50 μm diameter) phytoplankton enumerated by flow cytometry. However, at Stations 1 to 3, higher chlorophyll *a* was observed while INP freezing temperatures were relatively colder, which indicates that biomass alone is not a driver of atmospheric ice nucleation. In contrast, the contribution of small phytoplankton (particularly picoeukaryotes) was relatively low at Stations 1 to 3 (compare Figures 6 and S1).

Mayol et al. (2014) estimated aerosolization rates of microorganisms from the North Atlantic Ocean during summer to be 9 to 100 prokaryote cells m^{-2} s^{-1} and 0.01 to 0.1 eukaryote cells m^{-2} s^{-1}. Revisiting our central hypothesis, our results indicate that marine phytoplankton contribute to an effective population of atmospheric INPs. Moreover, our results suggest that smaller chlorophyll-containing cells (<50 μm) may be key contributors to freezing in atmospheric droplets.

Acknowledgments
We thank Joseph Niehaus for assistance in collecting samples, and the Captain and crew of the R.V. *Atlantis* for making this project possible. Financial support was provided by NSF ATM (Award 1539881) and NASA (Awards NNX15AE68G and NNX15AE66G). This is PMEL contribution 4926. Data presented in this manuscript are available through the Texas Data Repository (https://doi.org/10.18738/T8/NH1EFA), and the NASA NAAMES data archive (https://naames.larc.nasa.gov).

References

Aller, J. Y., Kuznetsova, M. R., Jahns, C. J., & Kemp, P. F. (2005). The sea surface microlayer as a source of viral and bacterial enrichment in marine aerosols. *Journal of Aerosol Science*, *36*, 801–812. https://doi.org/10.1016/j.jaerosci.2004.10.012

Aller, J. Y., Radway, J. C., Kilthau, W. P., Bothe, D. W., Wilson, T. W., Vaillancourt, R. D., et al. (2017). Size-resolved characterization of the polysaccharidic and proteinaceous components of sea spray aerosol. *Atmospheric Environment*, *154*, 331–347. https://doi.org/10.1016/j.atmosenv.2017.01.053

Alpert, P. A., Aller, J. Y., & Knopf, D. A. (2011a). Ice nucleation from aqueous NaCl droplets with and without marine diatoms. *Atmospheric Chemistry and Physics*, *11*(12), 5539–5555. https://doi.org/10.5194/acp-11-5539-2011

Alpert, P. A., Aller, J. Y., & Knopf, D. A. (2011b). Initiation of the ice phase by marine biogenic surfaces in supersaturated gas and supercooled aqueous phases. *Physical Chemistry Chemical Physics*, *13*(44), 19,882–19,894. https://doi.org/10.1039/c1cp21844a

Atkinson, J. D., Murray, B. J., Woodhouse, M. T., Whale, T. F., Baustian, K. J., Carslaw, K. S., & Malkin, T. L. (2013). The importance of feldspar for ice nucleation by mineral dust in mixed-phase clouds. *Nature*, *498*, 355–358. https://doi.org/10.1038/nature12278

Baer, S. E., Lomas, M. W., Terpis, K. X., Mouginot, C., & Martiny, A. C. (2017). Stoichiometry of *Prochlorococcus*, *Synechococcus*, and small eukaryotic populations in the western North Atlantic Ocean. *Environmental Microbiology*, *19*(4), 1568–1583. https://doi.org/10.1111/1462-2920.13672

Barbaro, E., Feltracco, M., Cesari, D., Padoan, S., Zangrando, R., Contini, D., et al. (2019). Characterization of the water soluble fraction in ultrafine, fine, and coarse atmospheric aerosol. *Science of the Total Environment*, *658*, 1423–1439. https://doi.org/10.1016/j.scitotenv.2018.12.298

Bates, T. S., Quinn, P. K., Frossard, A. A., Russell, L. M., Hakala, J., Petäjä, T., et al. (2012). Measurements of ocean derived aerosol off the coast of California. *Journal of Geophysical Research*, *117*, 148, D00V15–227. https://doi.org/10.1029/2012JD017588

Behrenfeld, M. J., Moore, R. H., Hostetler, C. A., Graff, J., Gaube, P., Russell, L. M., et al. (2019). The North Atlantic Aerosol and Marine Ecosystem Study (NAAMES): Science motive and mission overview. *Frontiers in Marine Science*, *6*, 122. https://doi.org/10.3389/fmars.2019.00122

Bettarel, Y., Kan, J., Wang, K., Williamson, K., Cooney, S., Ribblett, S., et al. (2005). Isolation and preliminary characterisation of a small nuclear inclusion virus infecting the diatom *Chaetoceros* cf. *gracilis*. *Aquatic Microbial Ecology*, *40*(2), 103–114. https://doi.org/10.3354/ame040103

Blanchard, D. C., & Woodcock, A. H. (1957). Bubble formation and modification in the sea and its meteorological significance. *Tellus*, *9*(2), 145–158. https://doi.org/10.3402/tellusa.v9i2.9094

Bodnar, R. (1993). Revised equation and table for determining the freezing point depression of H_2O-NaCl solutions. *Geochimica et Cosmochimica Acta*, *57*(3), 683–684. https://doi.org/10.1016/0016-7037(93)90378-A

Bratbak, G., Egge, J. K., & Heldal, M. J. M. E. P. S. (1993). Viral mortality of the marine alga *Emiliania huxleyi* (Haptophyceae) and termination of algal blooms. *Marine Ecology Progress Series*, *93*(1-2), 39–48. https://doi.org/10.3354/meps093039

Brooks, S. D., Suter, K., & Olivarez, L. (2014). Effects of chemical aging on the ice nucleation activity of soot and polycyclic aromatic hydrocarbon aerosols. *The Journal of Physical Chemistry A*, *118*(43), 10,036–10,047. https://doi.org/10.1021/jp508809y

Brooks, S. D., & Thornton, D. C. O. (2018). Marine aerosols and clouds. *Annual Review of Marine Science*, *10*(1), 289–313. https://doi.org/10.1146/annurev-marine-121916-063148

Chance, R. J., Hamilton, J. F., Carpenter, L. J., Hackenberg, S. C., Andrews, S. J., & Wilson, T. W. (2018). Water-soluble organic composition of the arctic sea surface microlayer and association with ice nucleation ability. *Environmental Science & Technology*, *52*(4), 1817–1826. https://doi.org/10.1021/acs.est.7b04072

Clarke, A. D., Owens, S. R., & Zhou, J. (2006). An ultrafine sea-salt flux from breaking waves: Implications for cloud condensation nuclei in the remote marine atmosphere. *Journal of Geophysical Research*, *111*, D06202. https://doi.org/10.1029/2005JD006565

Collier, K. N., & Brooks, S. D. (2016). Role of organic hydrocarbons in atmospheric ice formation via contact freezing. *The Journal of Physical Chemistry A*, *120*(51), 10,169–10,180. https://doi.org/10.1021/acs.jpca.6b11890

Creamean, J. M., Cross, J. N., Pickart, R., McRaven, L., Lin, P., Pacini, A., et al. (2019). Ice nucleating particles carried from below a phytoplankton bloom to the arctic atmosphere. *Geophysical Research Letters*, *46*, 8572–8581. https://doi.org/10.1029/2019GL083039

Cunliffe, M., Engel, A., Frka, S., Gasparovic, B., Guitart, C., Murrell, J. C., et al. (2013). Sea surface microlayers: A unified physicochemical and biological perspective of the air-ocean interface. *Progress in Oceanography*, *109*, 104–116. https://doi.org/10.1016/j.pocean.2012.08.004

DeMott, P. J. (1990). An exploratory study of ice nucleation by soot aerosols. *Journal of Applied Meteorology*, *29*(10), 1072–1079. https://doi.org/10.1175/15200450(1990)029<1072:AESOIN>2.0.CO;2

DeMott, P. J., Hill, T. C. J., McCluskey, C. S., Prather, K. A., Collins, D. B., Sullivan, R. C., et al. (2016). Sea spray aerosol as a unique source of ice nucleating particles. *Proceedings of the National Academy of Sciences*, *113*(21), 5797–5803. https://doi.org/10.1073/pnas.1514034112

Engel, A., Bange, H. W., Cunliffe, M., Burrows, S. M., Friedrichs, G., Galgani, L., et al. (2017). The ocean's vital skin: Toward an integrated understanding of the sea surface microlayer. *Frontiers in Marine Science*, *4*, 14. https://doi.org/10.3389/fmars.2017.00165

Failor, K. C., Schmale, D. G. III, Vinatzer, B. A., & Monteil, C. L. (2017). Ice nucleation active bacteria in precipitation are genetically diverse and nucleate ice by employing different mechanisms. *The ISME Journal*, *11*(12), 2740–2753. https://doi.org/10.1038/ismej.2017.124

Fall, R., & Schnell, R. C. (1985). Association of an ice-nucleating pseudomonad with cultures of the marine dinoflagellate, *Heterocapsa niei*. *Journal of Marine Research*, *43*(1), 257–265. https://doi.org/10.1357/002224085788437370

Fletcher, N. H. (1969). Active sites and ice crystal nucleation. *Journal of the Atmospheric Sciences*, *26*(6), 1266–1271. https://doi.org/10.1175/1520-0469(1969)026<1266:ASAICN>2.0.CO;2

Flombaum, P., Gallegos, J. L., Gordillo, R. A., Rincon, J., Zabala, L. L., Jiao, N. A. Z., et al. (2013). Present and future global distributions of the marine Cyanobacteria *Prochlorococcus* and *Synechococcus*. *Proceedings of the National Academy of Sciences of the United States of America*, *110*(24), 9824–9829. https://doi.org/10.1073/pnas.1307701110

Fornea, A. P., Brooks, S. D., Dooley, J. B., & Saha, A. (2009). Heterogeneous freezing of ice on atmospheric aerosols containing ash, soot, and soil. *Journal of Geophysical Research*, *114*, D13201. https://doi.org/10.1029/2009JD011958

Gobler, C. J., Hutchins, D. A., Fisher, N. S., Cosper, E. M., & Sañudo-Wilhelmy, S. A. (1997). Release and bioavailability of C, N, P Se, and Fe following viral lysis of a marine chrysophyte. *Limnology and Oceanography*, *42*(7), 1492–1504. https://doi.org/10.4319/lo.1997.42.7.1492

Graff, J. R., & Behrenfeld, M. J. (2018). Photoacclimation responses in subarctic Atlantic phytoplankton following a natural mixing-restratification event. *Frontiers in Marine Science*, *5*, 209. https://doi.org/10.3389/fmars.2018.00209

Graff, J. R., Milligan, A. J., & Behrenfeld, M. J. (2012). The measurement of phytoplankton biomass using flow-cytometric sorting and elemental analysis of carbon. *Limnology and Oceanography: Methods*, *10*(11), 910–920. https://doi.org/10.4319/lom.2012.10.910

Graff, J. R., Westberry, T. K., Milligan, A. J., Brown, M. B., Dall'Olmo, G., Dongen-Vogels, V., & Behrenfeld, M. J. (2015). Analytical phytoplankton carbon measurements spanning diverse ecosystems. *Deep Sea Research Part I: Oceanographic Research Papers*, *102*, 16–25. https://doi.org/10.1016/j.dsr.2015.04.006

Hader, J. D., Wright, T. P., & Petters, M. D. (2014). Contribution of pollen to atmospheric ice nuclei concentrations. *Atmospheric Chemistry and Physics*, *14*(11), 5433–5449. https://doi.org/10.5194/acp-14-5433-2014

Hooker, S. B., Van Heukelem, L., Thomas, C. S., Claustre H., Ras, J., Barlow, R., et al. (2005) The second SeaWIFS HPLC analysis round-robin experiment (SeaHARRE-2). NASA/TM–2005–212787. National Aeronautics and Space Administration, Goddard Space Flight Center, Greenbelt, Maryland.

Hoose, C., & Möhler, O. (2012). Heterogeneous ice nucleation on atmospheric aerosols: A review of results from laboratory experiments. *Atmospheric Chemistry and Physics*, *12*(20), 9817–9854. https://doi.org/10.5194/acp-12-9817-2012

Huang, W. T. K., Ickes, L., Tegen, I., Rinaldi, M., Ceburnis, D., & Lohmann, U. (2018). Global relevance of marine organic aerosols as ice nucleating particles. *Atmospheric Chemistry and Physics*, *18*(15), 11,423–11,445. https://doi.org/10.5194/acp-2017-922

Hunter, K. A. (1997). Chemistry of the sea-surface microlayer. In P. Liss & R. A. Duce (Eds.), *The Sea Surface and Global Change* (pp. 287–320). Cambridge: Cambridge University Press.

Irish, V. E., Elizondo, P., Chen, J., Chou, C., Charette, J., Lizotte, M., et al. (2017). Ice-nucleating particles in Canadian Arctic sea-surface microlayer and bulk seawater. *Atmospheric Chemistry and Physics*, *17*(17), 10,583–10,595. https://doi.org/10.5194/acp-17-10583-2017

Irish, V. E., Hanna, S. J., Xi, Y., Boyer, M., Polishchuk, E., Ahmed, M., et al. (2019). Revisiting properties and concentrations of ice-nucleating particles in the sea surface microlayer and bulk seawater in the Canadian Arctic during summer. *Atmospheric Chemistry and Physics*, *19*(11), 7775–7787. https://doi.org/10.5194/acp-19-7775-2019

Jiao, N., Herndl, G. J., Hansell, D. A., Benner, R., Kattner, G., Wilhelm, S. W., et al. (2010). Microbial production of recalcitrant dissolved organic matter: Long-term carbon storage in the global ocean. *Nature Reviews Microbiology*, *8*(8), 593–599. https://doi.org/10.1038/nrmicro2386

Kanji, Z. A., Ladino, L. A., Wex, H., Boose, Y., Burkert-Kohn, M., Cziczo, D. J., & Krämer, M. (2017). Overview of ice nucleating particles. *Meteorological Monographs*, *58*, 1.1–1.33. https://doi.org/10.1175/AMSMONOGRAPHS-D-16-0006.1

Kim, H., Orser, C., Lindow, S., & Sands, D. (1987). Xanthomonas campestris pv. translucens strains active in ice nucleation. *Plant Disease*, *71*(11), 994–997. https://doi.org/10.1094/PD-71-0994

Kiselev, A., Bachmann, F., Pedevilla, P., Cox, S. J., Michaelides, A., Gerthsen, D., & Leisner, T. (2017). Active sites in heterogeneous ice nucleation—The example of K-rich feldspars. *Science*, *355*(6323), 367–371. https://doi.org/10.1126/science.aai8034

Knopf, D. A., Alpert, P. A., Wang, B., & Aller, J. Y. (2011). Stimulation of ice nucleation by marine diatoms. *Nature Geoscience*, *4*(2), 88–90. https://doi.org/10.1038/NGEO1037

Komurcu, M., Storelvmo, T., Tan, I., Lohmann, U., Yun, Y. X., Penner, J. E., et al. (2014). Intercomparison of the cloud water phase among global climate models. *Journal of Geophysical Research: Atmospheres*, *119*, 3372–3400. https://doi.org/10.1002/2013jd021119

Koop, T., & Zobrist, B. (2009). Parameterizations for ice nucleation in biological and atmospheric systems. *Physical Chemistry Chemical Physics*, *11*(46), 10,839–10,850. https://doi.org/10.1039/B914289D

Kujawinski, E. B. (2011). The Impact of microbial metabolism on marine dissolved organic matter. *Annual Review of Marine Science*, *3*, 567–599. https://doi.org/10.1146/annurev-marine-120308-081003

Ladino, L. A., Yakobi-Hancock, J. D., Kilthau, W. P., Mason, R. H., Si, M., Li, J., et al. (2016). Addressing the ice nucleating abilities of marine aerosol: A combination of deposition mode laboratory and field measurements. *Atmospheric Environment*, *132*, 1–10. https://doi.org/10.1016/j.atmosenv.2016.02.028

Lenes, J. M., Walsh, J. J., & Darrow, B. P. (2013). Simulating cell death in the termination of *Karenia brevis* blooms: Implication for predicting aerosol toxicity vectors to humans. *Marine Ecology Progress Series*, *493*, 71–81. https://doi.org/10.3354/meps10515

Lindow, S., Arny, D., & Upper, C. (1978). *Erwinia herbicola*: A bacterial ice nucleus active in increasing frost injury to corn. *Phytopathology*, *68*(3), 523–527. https://doi.org/10.1094/Phyto-68-523

Liss, P. S., & Duce, R. A. (1997). Preface. In P. Liss & R. A. Duce (Eds.), *The sea surface and global change* (pp. xiii–xvi). Cambridge: Cambridge University Press.

Lohmann, U., Lüönd, F., & Mahrt, F. (2016). *An introduction to clouds from the microscale to climate* (1st ed.). Cambridge, UK: Cambridge University Press.

Mace, G. G. (2010). Cloud properties and radiative forcing over the maritime storm tracks of the Southern Ocean and North Atlantic derived from A-Train. *Journal of Geophysical Research*, *115*, D10201. https://doi.org/10.1029/2009jd012517

Maki, L. R., Galyan, E. L., Chang-Chien, M.-M., & Caldwell, D. R. (1974). Ice nucleation induced by *Pseudomonas syringae*. *Applied Microbiology*, *28*(3), 456–459. https://doi.org/10.1128/AEM.28.3.456-459.1974

Mason, R. H., Si, M., Chou, C., Irish, V. E., Dickie, R., Elizondo, P., et al. (2016). Size-resolved measurements of ice-nucleating particles at six locations in North America and one in Europe. *Atmospheric Chemistry and Physics*, *16*(3), 1637–1651. https://doi.org/10.5194/acp-16-1637-2016

Mayol, E., Jiménez, M. A., Herndl, G. J., Duarte, C. M., & Arrieta, J. M. (2014). Resolving the abundance and air-sea fluxes of airborne microorganisms in the North Atlantic Ocean. *Frontiers in Microbiology*, *5*, 557. https://doi.org/10.3389/fmicb.2014.00557

McCluskey, C. S., Hill, T. C. J., Malfatti, F., Sultana, C. M., Lee, C., Santander, M. V., et al. (2017). A dynamic link between ice nucleating particles released in nascent sea spray aerosol and oceanic biological activity during two mesocosm experiments. *Journal of the Atmospheric Sciences*, *74*(1), 151–166. https://doi.org/10.1175/JAS-D-16-0087.1

McCluskey, C. S., Ovadnevaite, J., Rinaldi, M., Atkinson, J., Belosi, F., Ceburnis, D., et al. (2018). Marine and terrestrial organic ice-nucleating particles in pristine marine to continentally influenced Northeast Atlantic air masses. *Journal of Geophysical Research: Atmospheres*, *123*, 6196–6212. https://doi.org/10.1029/2017JD028033

Møller, E. F. (2007). Production of dissolved organic carbon by sloppy feeding in the copepods *Acartia tonsa, Centropages typicus*, and *Temora longicornis*. *Limnology and Oceanography*, *52*(1), 79–84. https://doi.org/10.4319/lo.2007.52.1.0079

Møller, E. F., Thor, P., & Nielsen, T. G. (2003). Production of DOC by *Calanus finmarchicus, C. glacialis* and *C. hyperboreus* through sloppy feeding and leakage from fecal pellets. *Marine Ecology Progress Series*, *262*, 185–191. https://doi.org/10.3354/meps262185

Mueller, J., Pietras, C., Hooker, S., Clark, D., Frouin, A. M. R., & Fargion, G. (2002). Ocean optics protocols for satellite ocean color sensor validation, revision 3, volumes 1 and 2. *NASA technical memo,* doi:10.25607/OBP-62

Murray, B. J., O'Sullivan, D., Atkinson, J. D., & Webb, M. E. (2012). Ice nucleation by particles immersed in supercooled cloud droplets. *Chemical Society Reviews*, *41*(19), 6519–6554. https://doi.org/10.1039/C2CS35200A

Murray, B. J., Wilson, T. W., Dobbie, S., Cui, Z. Q., Al-Jumur, S., Möhler, O., et al. (2010). Heterogeneous nucleation of ice particles on glassy aerosols under cirrus conditions. *Nature Geoscience*, *3*(4), 233–237. https://doi.org/10.1038/ngeo817

O'Dowd, C. D., Ceburnis, D., Ovadnevaite, J., Bialek, J., Stengel, D. B., Zacharias, M., et al. (2015). Connecting marine productivity to sea-spray via nanoscale biological processes: Phytoplankton dance or death disco? *Scientific Reports*, *5*(1), 14883. https://doi.org/10.1038/srep14883

Partensky, F., Blanchot, J., & Vaulot, D. (1999). Differential distribution and ecology of *Prochlorococcus* and *Synechococcus* in oceanic waters: A review. In L. Charpy & A. Larkum (Eds.), *Marine Cyanobacteria* (pp. 457–475). Monaco: Musée Océanographique.

Pummer, B., Bauer, H., Bernardi, J., Bleicher, S., & Grothe, H. (2012). Suspendable macromolecules are responsible for ice nucleation activity of birch and conifer pollen. *Atmospheric Chemistry and Physics*, *12*(5), 2541–2550. https://doi.org/10.5194/acp-12-2541-2012

Rahlff, J. (2019). The virioneuston: A review on viral-bacterial associations at air-water interfaces. *Viruses-Basel*, *11*(2), 13. https://doi.org/10.3390/v11020191

Rosinski, J., Haagenson, P., Nagamoto, C., & Parungo, F. (1986). Ice-forming nuclei of maritime origin. *Journal of Aerosol Science*, *17*(1), 23–46. https://doi.org/10.1016/0021-8502(86)90004-2

Rosinski, J., Haagenson, P., Nagamoto, C., & Parungo, F. (1987). Nature of ice-forming nuclei in marine air masses. *Journal of Aerosol Science*, *18*(3), 291–309. https://doi.org/10.1016/0021-8502(87)90024-3

Russell, L. M., Hawkins, L. N., Frossard, A. A., Quinn, P. K., & Bates, T. S. (2010). Carbohydrate-like composition of submicron atmospheric particles and their production from ocean bubble bursting. *Proceedings of the National Academy of Sciences*, *107*(15), 6652–6657. https://doi.org/10.1073/pnas.0908905107

Schnell, R. C., & Vali, G. (1975). Freezing nuclei in marine waters. *Tellus*, *27*(3), 321–323. https://doi.org/10.1111/j.2153-3490.1975.tb01682.x

Schnell, R. C., & Vali, G. (1976). Biogenic ice nuclei: Part I. Terrestrial and marine sources. *Journal of the Atmospheric Sciences*, *33*(8), 1554–1564. https://doi.org/10.1175/1520-0469(1976)

Shaw, R. A., Durant, A. J., & Mi, Y. J. (2005). Heterogeneous surface crystallization observed in undercooled water. *Journal of Physical Chemistry B*, *109*(20), 9865–9868. https://doi.org/10.1021/jp0506336

Shuter, B. (1979). A model of physiological adaptation in unicellular algae. *Journal of Theoretical Biology*, *78*, 519–552. https://doi.org/10.10/0022-5193(79)90189-9

Sieburth, J. M., Smetacek, V., & Lenz, J. (1978). Pelagic ecosystem structure: Heterotrophic compartments of the plankton and their relationship to plankton size fractions 1. *Limnology and Oceanography*, *23*(6), 1256–1263. https://doi.org/10.4319/lo.1978.23.6.1256

Stratmann, F., & Wiendensohler, A. (1996). A new data inversion algorithm for DMPS measurements. *Journal of Aerosol Science Supplement*, *27*(1), 339–340. https://doi.org/10.1016/0021-8502(96)00242-X

Thornton, D. C. O. (2014). Dissolved organic matter (DOM) release by phytoplankton in the contemporary and future ocean. *European Journal of Phycology*, *49*(1), 20–46. https://doi.org/10.1080/09670262.2013.875596

Thornton, D. C. O., Brooks, S. D., & Chen, J. (2016). Protein and carbohydrate exopolymer particles in the sea surface microlayer (SML). *Frontiers in Marine Science*, *3*, 135. https://doi.org/10.3389/fmars.2016.00135

Turnbull, D., & Vonnegut, B. (1952). Nucleation catalysis. *Industrial and Engineering Chemistry*, *44*(6), 1292–1298. https://doi.org/10.1021/ie50510a031

Vali, G., DeMott, P., Möhler, O., & Whale, T. (2015). A proposal for ice nucleation terminology. *Atmospheric Chemistry and Physics*, *15*(18), 10,263–10,270. https://doi.org/10.5194/acp-15-10263-2015

Van Heukelem, L., & Thomas, C. S. (2001). Computer-assisted high-performance liquid chromatography method development with applications to the isolation and analysis of phytoplankton pigments. *Journal of Chromatography A*, *910*(1), 31–49. https://doi.org/10.1016/S0378-4347(00)00603-4

Wallace, J. M., & Hobbs, P. V. (2006). *Atmospheric science: An introductory survey* (2nd ed.). Amsterdam; Boston: Elsevier Academic Press.

Wex, H., Augustin-Bauditz, S., Boose, Y., Budke, C., Curtius, J., Diehl, K., et al. (2015). Intercomparing different devices for the investigation of ice nucleating particles using Snomax® as test substance. *Atmospheric Chemistry and Physics*, *15*(3), 1463–1485. https://doi.org/10.5194/acp-15-1463-2015

Whale, T. F., Holden, M. A., Wilson, T. W., O'Sullivan, D., & Murray, B. J. (2018). The enhancement and suppression of immersion mode heterogeneous ice-nucleation by solutes. *Chemical Science*, *9*(17), 4142–4151. https://doi.org/10.1039/C7SC05421A

Wilson, T. W., Ladino, L. A., Alpert, P. A., Breckels, M. N., Brooks, I. M., Browse, J., et al. (2015). A marine biogenic source of atmospheric ice-nucleating particles. *Nature*, *525*(7568), 234–238. https://doi.org/10.1038/nature14986

Wolf, M. J., Coe, A., Dove, L. A., Zawadowicz, M. A., Dooley, K., Biller, S. J., et al. (2019). Investigating the heterogeneous ice nucleation of sea spray aerosols using *Prochlorococcus* as a model source of marine organic matter. *Environmental Science & Technology*, *53*(3), 1139–1149. https://doi.org/10.1021/acs.est.8b05150

Yun, Y. X., & Penner, J. E. (2013). An evaluation of the potential radiative forcing and climatic impact of marine organic aerosols as heterogeneous ice nuclei. *Geophysical Research Letters*, *40*, 4121–4126. https://doi.org/10.1002/grl.50794

Zeppenfeld, S., van Pinxteren, M., Hartmann, M., Bracher, A., Stratmann, F., & Herrmann, H. (2019). Glucose as a potential chemical marker for ice nucleating activity in Arctic seawater and melt pond samples. *Environmental Science & Technology*, *53*(15), 8747–8756. https://doi.org/10.1021/acs.est.9b01469